Experimental and Theoretical Investigation of Minimization of Forming-Induced Variability in Resistive Memory Devices

Brian L. Geist[1], Dmitri Strukov[2] and Vladimir Kochergin[1]
[1]MicroXact, Inc., Blacksburg, VA 24060-6376, U.S.A.
[2]Electrical and Computer Engineering Department, UC Santa Barbara, Santa Barbara, CA 93106-9560, U.S.A.

ABSTRACT

Resistive memory materials and devices (often called memristors) are an area of intense research, with metal/metal oxide/metal resistive elements a prominent example of such devices. Electroforming (the formation of a conductive filament in the metal oxide layer) represents one of the often necessary steps of resistive memory device fabrication that results in large and poorly controlled variability in device performance. In this contribution we present a numerical investigation of the electroforming process. In our model, drift and Ficks and Soret diffusion processes are responsible for movement of vacancies in the oxide material. Simulations predict filament formation and qualitatively agreed with a reduction of the forming voltage in structures with a top electrode. The forming and switching results of the study are compared with numerical simulations and show a possible pathway toward more repeatable and controllable resistive memory devices.

INTRODUCTION

Resistive memory materials and devices (often called memristors) are an area of intense research, due to the enormous promise that such devices hold for digital data storage and processing applications. A memristor [1,2] is a 2-terminal electrical circuit element that changes its resistance depending on the position of vacancies inside the device which can form a filament through electroforming. [3] Typically, a memristor is made of a specific thin film material sandwiched between two metallic electrodes (wires). The resistance of a thin film can be switched either in continuous or binary fashion by applying a voltage to the electrodes.

At present, despite of significant progress made to date, the understanding of resistive switching (forming, as well as the processes taking place during set and reset operations) is still not fully developed. Recently, the numerical reset model based on temperature/field-driven ion migration in metal-oxide-metal memristive devices was suggested. [4] In this contribution we significantly expand the model by including a thermophoresis contribution and by modeling not only the reset process but also the device forming process.

THEORY

Development of a solid model with cylindrical symmetry

Titanium oxide was chosen as the modeling material in order to analyze the predicted behavior of memristor devices. The electrical and thermal properties of titanium oxide are already well established [5] which allow for the material to be modeled using COMSOL®. Pure titanium dioxide has a much higher resistivity relative to Magnèli phases of titanium oxide compared to what has been reported for hafnium dioxide [4] making it a more suitable candidate for studying the filament forming process.

Memristive behavior can be modeled as a function of three coupled variables; the density of oxygen vacancies N, the applied voltage V and the temperature T. Filaments form via the movement of oxygen vacancies inside the material which when reaching a sufficient density in a particular region can turn titanium oxide from resistive to conductive. The movement of vacancies has been modeled using the drift-diffusion equation containing terms for both Fick and Soret diffusion as thermophoresis [6] has recently been proposed as a mechanism for vacancy movement:

$$\frac{\partial N}{\partial t} - \nabla \cdot c\overrightarrow{\nabla N} - \nabla \cdot \vec{\alpha} N - \mathrm{a}N = 0$$

where $\mathrm{c} = \mathrm{D_0 e^{-E_A/k_b T}}$ is the Fick diffusion coefficient, $\vec{\alpha} = \frac{\mathrm{q D_0 e^{-E_A/k_b T}} \overrightarrow{\nabla V}}{\mathrm{k_b T}}$ is the drift coefficient and $\mathrm{a} = \frac{\mathrm{D_0 e^{-E_A/k_b T} E_A} \overrightarrow{\nabla T}}{\mathrm{k_b T^2}}$ is the Soret diffusion coefficient. Inside the coefficients, $\mathrm{D_0}$ is the diffusivity constant, E_A is the energy barrier height, k_b is Boltzmann's constant, q is the elementary charge, $\overrightarrow{\nabla V}$ is the potential gradient and T is the temperature.

Electrical conductivity in titanium oxide has been modeled from the carrier continuity equation:

$$\nabla \cdot \mathrm{c}\overrightarrow{\nabla \mathrm{V}} = 0$$

where $\mathrm{c} = -\sigma_0 \mathrm{e^{-E_{AC}(N)/k_b T}}$ with σ_0 being the conductivity coefficient and E_{AC} being the electronic activation energy as a function of localized vacancy density N. Based on data reported by Harada, *et al*, [5] σ_0 and E_{AC} were modeled as functions of vacancy density.

Thermal conductivity is coupled to the electrical conductivity through the steady-state Fourier equation:

$$-\nabla \cdot c\overrightarrow{\nabla T} = f$$

where $c = k_{th}$ is the thermal conductivity and is also modeled from data presented by Harada, *et al*. [5] $f = \sigma\left|\overrightarrow{\nabla V}(r,z)\right|^2$ is the forced response or the source term. The steady-state solution was chosen because of the time scale of the simulation. By modeling the equations in this format, they fit directly into COMSOL Multiphysics 4.3 Coefficient Form PDE module.

A two dimensional axis-symmetric geometry was chosen with platinum electrodes on the top and bottom of a titanium oxide layer. The top electrode was formed with a small protrusion into the titanium oxide layer in order to control the location of filament formation as displayed in the vacancy distribution shown in **Figure 1**. A voltage profile was applied across the electrodes with a dwell time at the end with no potential applied to monitor lagging thermal effects on the vacancy distribution. Continuous first derivative smoothing was applied to the voltage profile to avoid computational anomalies.

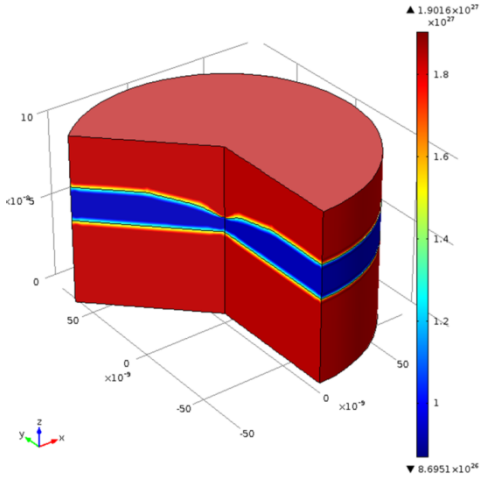

Figure 1: Cylindrical geometry chosen with a titanium oxide layer between platinum electrodes. Distances shown are in meters (m) and the color map displays oxygen vacancy distribution in m^{-3}.

Several assumptions were made to assist convergence of the COMSOL model. These were implemented in the Coefficient Form PDE module under Initial Values and Dirichlet Boundary Conditions. The top and bottom of the geometry as well as the initial temperature throughout the device were constrained to 300K. The platinum electrodes were assumed to be oxygen free and the movement of vacancies in platinum was heavily damped. Several different mesh sizes were analyzed with smaller mesh elements performing better in general but also taking longer to run than larger mesh elements.

A time dependent solver was chosen and the Relative tolerance in the Study Settings of the solver under Study 1 was enabled with a value of 0.01. The default solver uses a variable step size backward differentiation formula (BDF) which can artificially dampen large gradients. The solver was changed to a generalized-α method which is able to handle much sharper gradients without undue damping. The Direct Linear solver was set to MUltifrontal Massively Parallel sparse direct Solver (MUMPS) using an Automatic Nonlinear Newton's Method with an initial damping factor of 1 and the termination technique set to tolerance with a factor of 1. Other solver settings were left at their default values.

EXPERIMENT

Filament formation modeling

A series of simulations were run with different voltage magnitudes in order to study filament formation. Filaments form through a process of vacancy migration controlled by ion drift and diffusion and the electrical and thermal properties of the base material. **Figure 2** displays the filament formation under two different potentials.

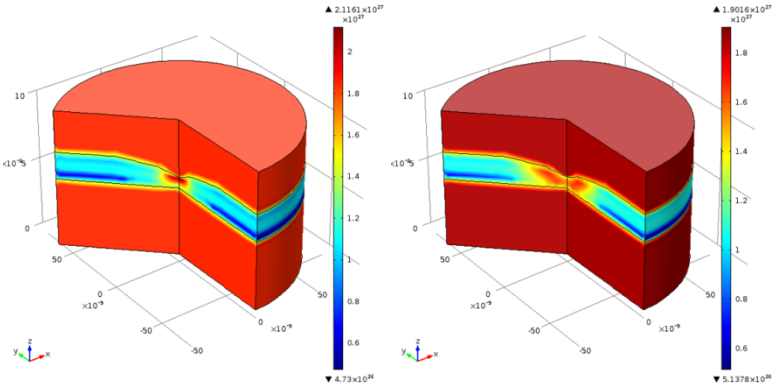

Figure 2: Vacancy distributions displaying filament formation at 1.545 V (left) and at 2 V (right).

I-V curves were generated for various potentials from 1 to 2 V. For smaller potentials, the material behaved in an ohmic fashion as shown in (a) of **Figure 3**. At 1.54 V as shown in (b), there is just a hint of vacancy migration visible at the high potentials. An increase of 5 mV as displayed in (c) allows for filament formation creating a hysteresis loop. It is interesting to note that at this filament formation threshold, the vacancies migrate after the voltage peak due to the thermal lag in the system. This leads to rounded top edge where the system does not reach a full set state (i.e. the current at 1 V is only 78% of the current at 1 V for a fully set filament created using 2 V as displayed in (d). Soret diffusion for highly non-stoichiometric TiO_x was found to have a minimal effect on the model with most simulations having less than a 1.5% decrease in forming voltage.

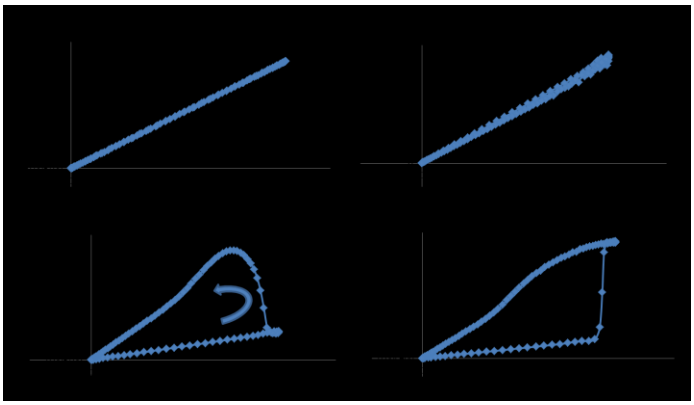

Figure 3: I-V curves for different applied potentials.

Testing demonstrates the possibility of an analog device

The application of successive voltage peaks provides a computational basis for an analog memristor. An analog memristor is a device that can predictably produce various currents with the same applied voltage depending on accumulation of vacancies to form a filament. **Figure 4** displays five different states achieved within a 300 nanosecond time frame by applying a series of voltage peaks. The memristor was reliably locked at a particular resistivity for voltages below 1.4 V and the differences in currents produced were enough to easily discriminate between settings.

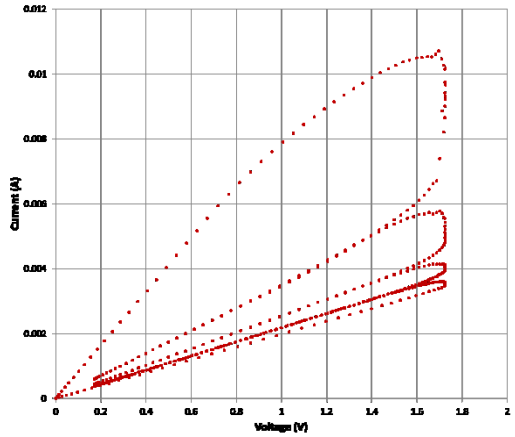

Figure 4: Titanium oxide memristor exhibiting multiple set states.

Memristors were fabricated by creating a protrusion from the top electrode across a titanium oxide layer similar to the model. Tunneling electron microscopy (TEM) was used to characterize the protrusion as displayed in **Figure 5**. The performance of the memristors can be observed in **Figure 6**. The switching occurs when a filament forms sharply decreasing the resistance of the device.

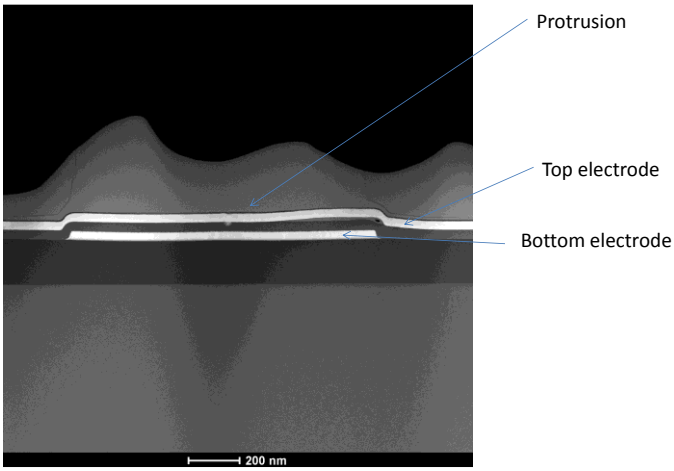

Figure 5 TEM image of the cross-section of ALD TiO_2-based memristor with e-beam defined protrusion as an artificial filament.

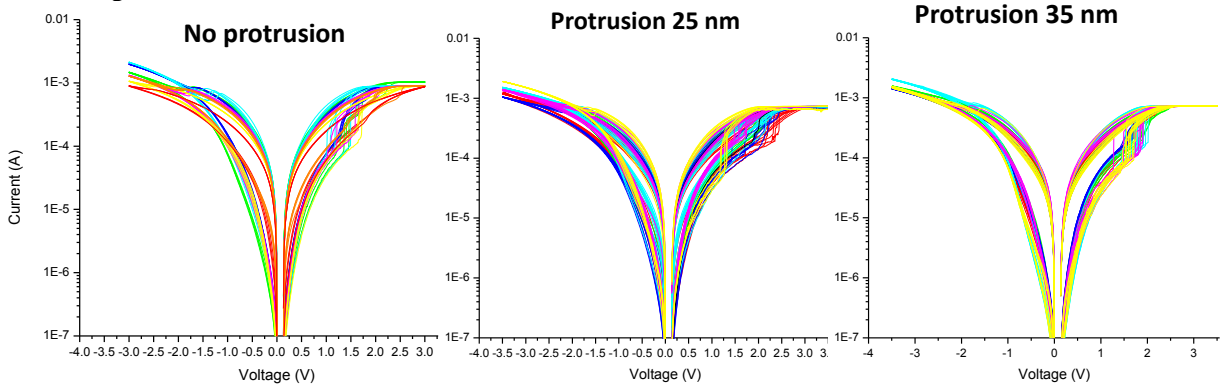

Figure 6 Forming of TiO_x-based memristors—each line displayed represents a forming curve. The number of devices exhibiting switching behavior increases as the depth of the

protrusion increases (about a 65% yield for no protrusion, 83% yield with a 25 nm protrusion and about a 94% yield with a 35 nm protrusion).

CONCLUSIONS

There are some improvements that can be made to the model. Currently all forming is voltage controlled due to the ease of implementing a voltage profile using COMSOL. In practice, current control is used to electroform filaments as it is easier to prevent runaway currents which would destroy the device as it becomes conductive. However, voltage control can be used to model the electroforming behavior of memristors.

The experimental results compared closely to the model with switching voltages between 1-2 V for the geometry chosen. The currents in the conductive state also agreed closely with the model while the model predicted higher than realized conductivities for the off state due to using highly non-stoichiometric TiO_x for the resistive element in the device to increase stability in the model. Future improvements to the model can be made by adding temperature dependence to the materials used and by developing current-controlled forming to prevent runaway conditions.

ACKNOWLEDGMENTS

The authors are grateful to Dr. Joseph E. Van Nostrand of AFRL/RITC for funding and for guidance of this effort (Phase I STTR contract FA8750-12-C-0157, Phase II STTR contract FA9550-11-C-0018).

REFERENCES

1. L.O. Chua, “Memristor - the missing circuit element,” IEEE Trans. Circuit Theory, vol. 18, 507–519, 1971.
2. D.B. Strukov, G. Snider, D.R. Stewart, and R.S. Williams, “The missing memristor found”, Nature 453, pp. 80-83, 2008.
3. J. Yang, F. Miao, M. Pickett, D. Ohlberg, D.R. Stewart, C. Lau, and R.S. Williams, “The mechanism of electroforming of metal oxide memristive switches,” Nanotechnology, vol. 20, no. 21, 2009.
4. S. Larentis, F. Nardi, S. Balatti, D. C. Gilmer, and D. Ielmini, "Resistive switching by voltage-driven ion migration in bipolar RRAM─ Part II: Modeling", IEEE Trans. Electron Devices, vol. 59, pp. 2468-2475 2012.
5. S. Harada, K. Tanaka, and H. Inui, “Thermoelectric properties and crystallographic shear structures in titanium oxides of the Magneli phases,” J. Appl. Phy., vol. 108, no. 8, 2010.
6. D.B. Strukov, F. Alibart, and R.S. Williams, “Thermophoresis/diffusion as the plausible mechanism for unipolar resistive switching in metal-oxide-metal memristors,” Appl. Phys. A, vol. 107, no. 3, pp. 509–518, 2012.